Electronic Supplementary Material (ESI) for Journal of Materials Chemistry A. This journal is © The Royal Society of Chemistry 2021

Two-dimensional MOF based Liquid Marbles: Surface Energy Calculations and Efficient Oil-Water Separation Using a ZIF-9-III@PVDF Membrane

Haneesh Saini, Parashuram Kallem, Eva Otyepková, Florian Geyer, Andreas Schneemann, Vaclav Ranc, Fawzi Banat, Radek Zbořil, Michal Otyepka,*Roland A. Fischer* and Kolleboyina Jayaramulu*

1. Characterization

The synthesized materials were characterized by different techniques. X-ray diffraction (XRD) data of all samples were collected by the X'Pert PRO PANanalytical equipment (Bragg-Brentano geometry with automatic divergence slits, position sensitive detector, continuous mode, room temperature, Cu-Kα radiation, Ni filter. The powder samples were dropped onto silicon wafer with grease, and measured at the same equipment (5-80°, at a step of 0.0197°, with accumulation time 200 s per step). The morphology and porous nature characterized through scanning electron microscopy (FESEM-FEI Nova-Nano SEM-600) and transmission electron microscope (JEOL JEM-3010 with accelerating voltage at 300 kV). The Raman spectra were recorded in backscattering arrangement, using 532 nm laser excitation using 6 mW laser power. Transmission electron microscopy (TEM) including high-resolution TEM analysis was performed using a FEI Tecnai G2 microscope. Selected-areaelectron diffraction patterns (SAED) were analyzed and fast Fourier transform (FFT) patternswere processed by using the Gatan Digital Micrograph software. SEM analysis of fabricated membranes, a sample of the membrane piece was coated with a 10 nm gold/platinium layer using a sputtering coating machine, and the analysis was preformed via Quanta 250 ESEM. The water content after filtration was tested by Karl Fischer moisture analyzer (Metrohm 851 Titrando system). The X-ray diffraction patterns of as-synthesized bulk and exfoliated samples of MOF were refined using GSAS software to determine the phase purity.

2. Contact Angle Measurements

For measuring contact angles, ZIF-9-III powder was pressed and flattened on a tape using a spatula and ZIF-9-I were pressed using a P/O/Weber 40E press. Advancing contact angles were measured using a Data Physics OCA35 contact angle goniometer with Data Physics SCA 20 software. First, 6 μL water droplets were deposited on the tablets. Afterwards, 15 μL of water was added to and removed from the drop. The measurement was performed at least three different spots per tablet. The error of the advancing contact angle measurements was estimated to be ±4 degrees.

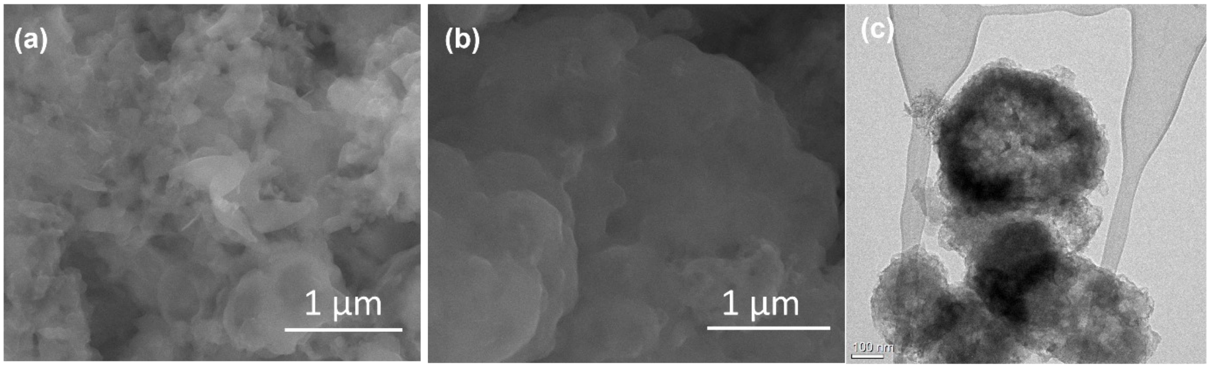

Fig. S1: (a-b) SEM (c) TEM images of bulk ZIF-9-III prepared through mechanochemical grinding

Discussion: Field emission scanning electron microscopy (FESEM) characterization reveals grinded bulk ZIF-9-III shows bundle of crystalline plates and Transmission electron microscopy (TEM) confirms the existence of stacked nanosheets

Table S1 Rietveld refinement parameters of bulk ZIF-9-III obtained from the powder diffraction data at room temperature. The numbers in parentheses are the estimated standard deviations of the last significant figure.

Compound	**MOF**
Space group	**C2/c**
composition	**-------**
***a*/Å**	**16.04(12)**
***b*/Å**	**16.14(9)**
***c*/Å**	**19.61(8)**
***V*/Å^3**	**5063.91(5)**
R_{wp}	**2.73%**
χ^2	**1.5**

Table S2 Rietveld refinement parameters of ZIF-9-III after exfoliation obtained from the powder diffraction data at room temperature. The numbers in parentheses are the estimated standard deviations of the last significant figure.

Compound	**ZIF-9-III-Exfoliated**
Space group	C2/c
composition	-------
a/Å	15.87(6)
b/Å	16.18(12)
c/Å	19.42(18)
V/Å^3	4986.25(2)
R_{wp}	2.43%
χ^2	1.2

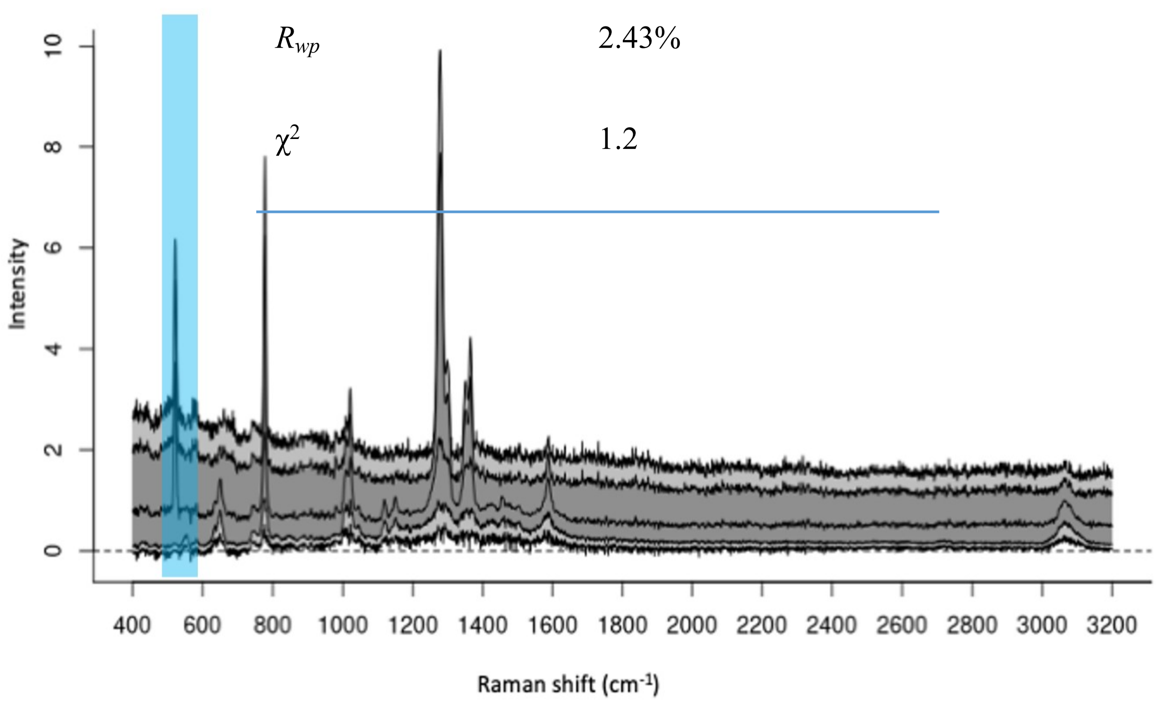

Fig. S2: Raman Spectrum of exfoliated ZIF-9-III

Discussion: Raman spectrum, where Co-N band is present at 464 cm-1. The Fig. shows clear existence of strong band 464 cm^{-1}.

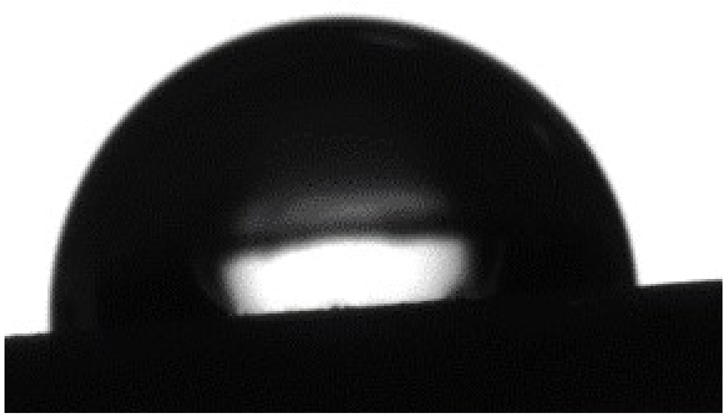

Fig. S3: Optical photograph of a water droplet (6μL) on pressed pellet of ZIF-9-I phase, showing contact angle around 92 ± 3°

Table S3: List of samples, their weights and specific surface areas.

Sample	Mass (mg)	Specific Surface area (m^2/g)
ZIF-9-I	6.4	450
ZIF-9-III	28.1	19

Discussion: The ZIF-9-1 is 3D structure with micro porous channels (Fig. 1a) and showing micro porous behavior having surface area around 450 m2/g with micro pore distribution, whereas ZIF-9-III phase non-porous two-dimensional layer with the surface area around 19 m2/g with meso pore distribution. These meso pores might be originated randomly ordered nanosheets [1]

Reference.

1.K. Jayaramulu, J. Masa, D.M. Morales, O. Tomanec, V. Ranc, M. Petr, P. Wilde, Y.-T. Chen, R. Zboril, W. Schuhmann, R.A. Fischer, Adv. Sci. 2018, 5, 1801029

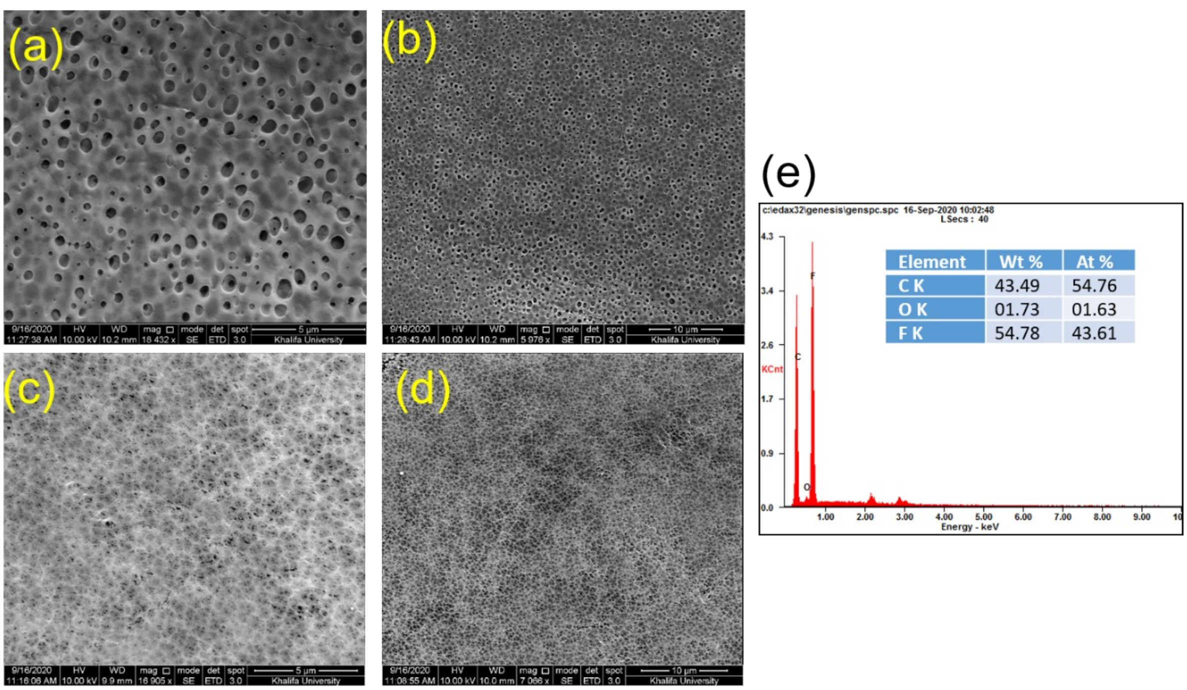

Fig. S4. SEM images of PVDF membrane (a-b) bottom view (c-d) top view; (e) EDS analysis

Discussion:

The SEM images of prepared pristine PVDF and ZIF-9-III/PVDF membranes (Fig. 5 b-e and Fig. S4) resembles the standard ultrafiltration membranes with no defects. From the SEM images of ZIF-9-III/PVDF (Fig. 5 b-c), it is clearly seen that ZIF-9-III particles were dispersed uniformly within the membranes. From the porosity measurements, it was observed that the bulk porosity decreased from 67.6 ± 3% of pristine PVDF membrane to 57.1 ± 2% of ZIF-9-III/PVDF membrane, thus it deteriorates the water flux slightly.

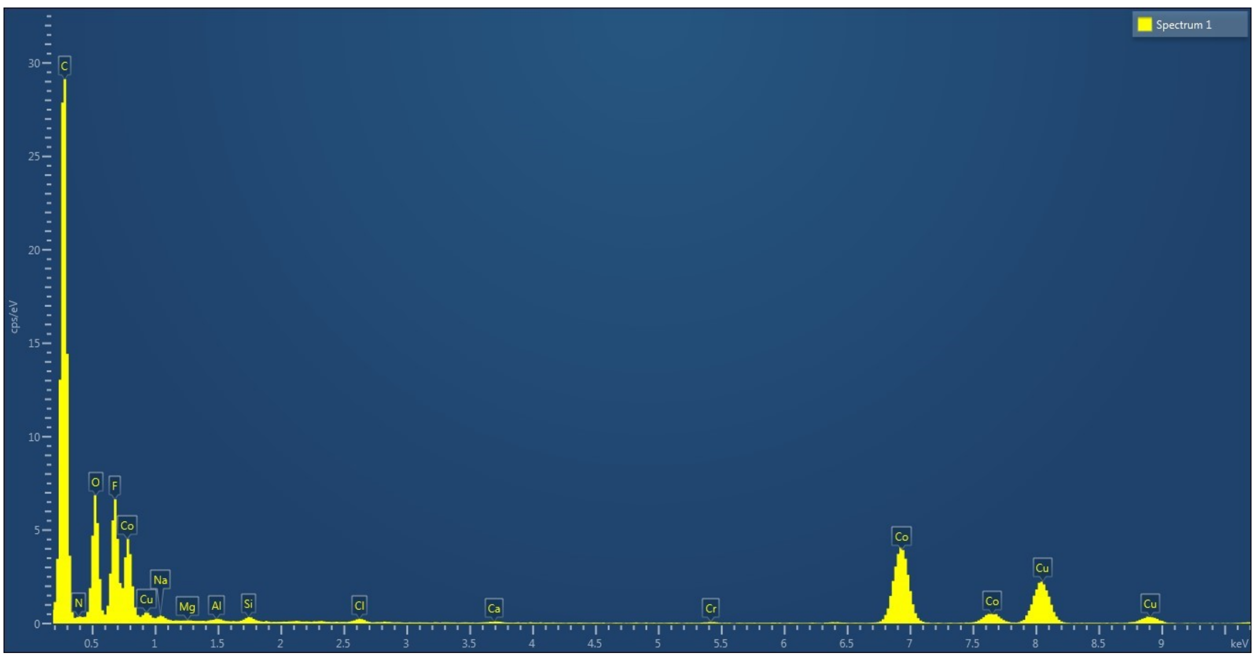

Fig. S5: EDS analysis of ZIF-9-III showing presence of Carbon, nitrogen, Cobalt, Oxygen and Fluorine elements of resultant membrane.

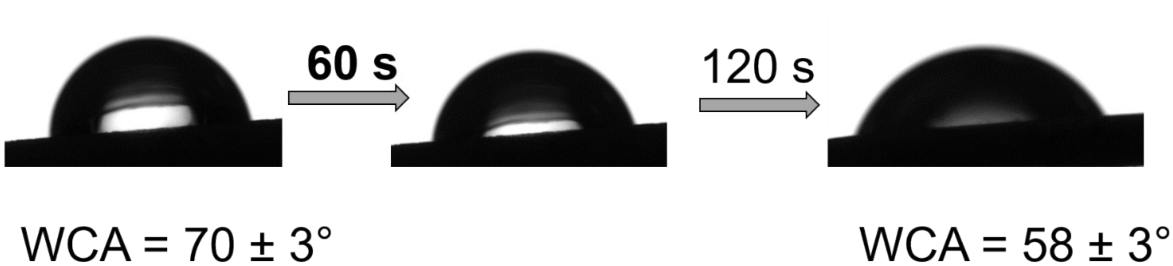

Fig. S6: Optical photograph of water droplet (6µL) on a PVDF membrane

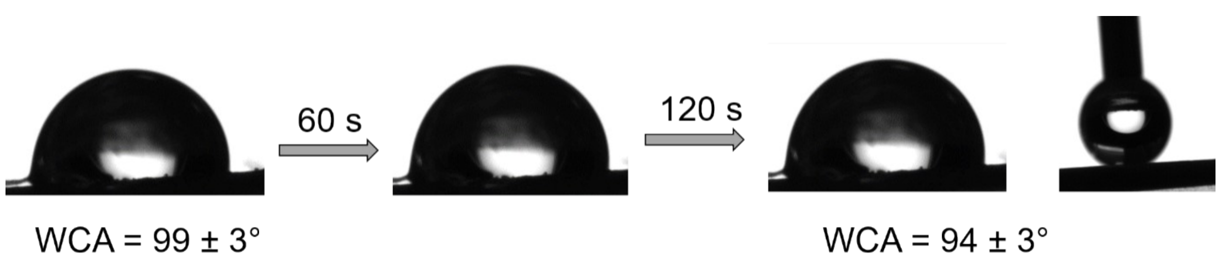

Fig. S7: Optical photograph of a water droplet (6µL) on a ZIF-9-@PVDF membrane

Discussion: The wettability of pristine PVDF and ZIF-9-III@PVDF membrane surfaces were investigated by static water contact angle (WCA) measurements. As observed in Fig. S6, the water droplet spread out on pristine PVDF membrane and the WCA decreased from 70 ± 3° to 58 ± 3° within 120 s. It was worth noting that the ZIF-9-III@PVDF membrane (Fig. S7) showed a WCA about 99 ± 3° and, after 120 s, the membrane presented WCA about 94 ± 3° with no deformation of droplet, indicating hydrophobicity.

Table S4 List of limiting values ($\nu \rightarrow 100\%$) of the total free surface energy ($\gamma_{1,t}$), its dispersive ($\gamma_{1,D}$) and acid-base ($\gamma_{1,AB}$) components (as percentage of the total surface free energy) and interfacial free energies of the ZIF-9-I and ZIF-9-III samples to water ($\gamma_{i,water}$) and n-hexane ($\gamma_{i,hexane}$)

Sample	Surface Area (m2/g)	$\gamma_{1,t}$ [mJ/m^2]	$\gamma_{1,AB}$ [%]	$\gamma_{1,D}$ [%]	$\gamma_{i,water}$ [mJ/m^2]	$\gamma_{i,hexane}$ [mJ/m^2]
ZIF-9-I	450	89 ± 4	11	89	34	31
ZIF-9-III	19	102 ± 6	9	91	42	38

Table S5: Compositions of the casting solutions used to fabricate MOF/PVDF membranes

Membrane code	**PVDF (wt%)**	**PVP (wt%)**	**ZIF-9-III * (wt%)**	**NMP (wt%)**
PVDF	16	2	0	82.0
ZIF-9-III@PVDF	16	2	2	81.84

*The percentage of **ZIF-9-III** is with respect to the total mass of PVDF in the casting solutions

Table S6: Oil-Water Separation efficiency of PVDF and ZIF-9-III@PVDF membranes

Membrane	Flux (L/m^2 h)	Water content (ppm) in the permeate	Rejection (%)
PVDF	17.5	960	74.02
ZIF-9-III@PVDF	14.3	6	99.8

Note: Water content in Oil/water emulsion of feed is 3724 ppm

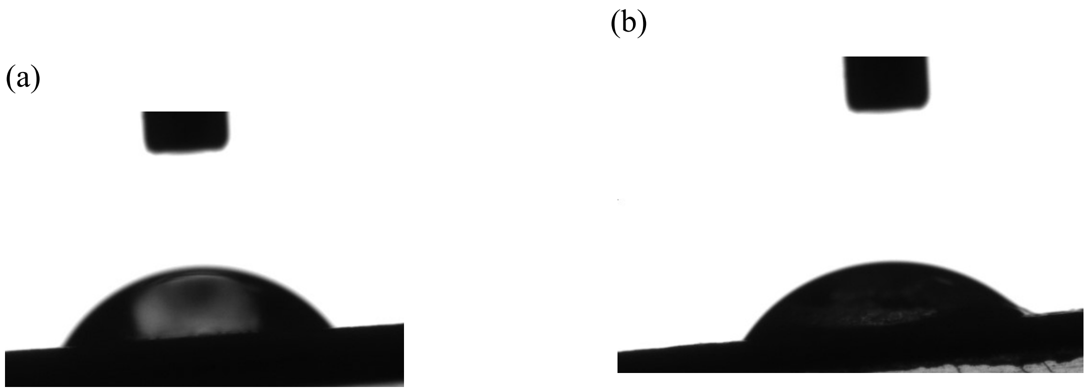

Fig. S8. Optical photograph of oil droplet on ZIF-9-III/PVDF membrane (a) vegetable oil, (b) Heptane.

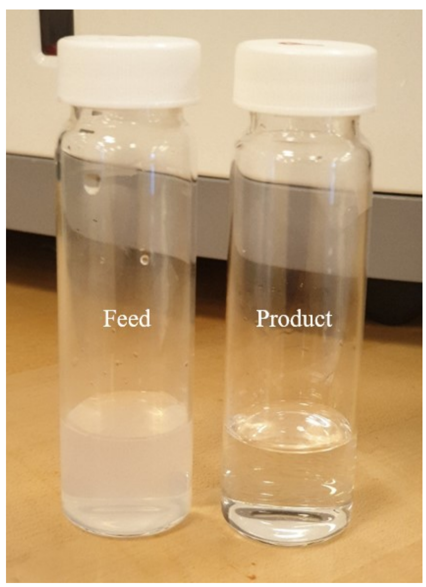

Fig. S9: Picture of oil/water emulsion (feed) and membrane purified oil (product).

Discussion: As shown in Fig. S9, the feed oil/water emulsion solution is non-transparent and become transparent (product) after permeating through ZIF-9-III@PVDF membrane.

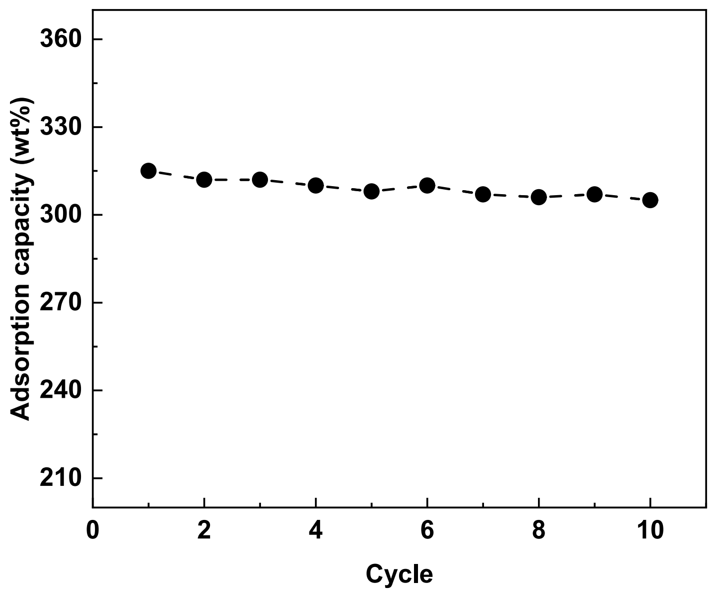

Fig. S10: Adsorption capacity of the ZIF-9-III@PVDF membrane over ten subsequent cycles and clearly shows significant adsorption capacity after 10 cycles of adsorption of vegetable oil.

<u>Table S7.</u> Tensile properties of pristine PVDF and ZIF-9-III@PVDF membranes.

Membrane	Tensile strength (MPa)	Elongation at break (%)
Pristine PVDF	1.83	28.9
ZIF-9-III@PVDF	2.24	29.7

Discussion: Mechanical properties were measured using Instron, Model No. 5982, USA) by performing tensile strength tests on membrane strips to the breaking point. The results of the tensile strength properties of the membranes are listed in the Table. The addition of ZIF-9- III increased the tensile strength of the PVDF membrane from 1.83 MPa to 2.14 MPa, while the elongation at break increased from 28.9% to 29.7%, indicating that ZIF-9- III may have contributed to the membrane's ability to withstand for long-term and harsh environments.

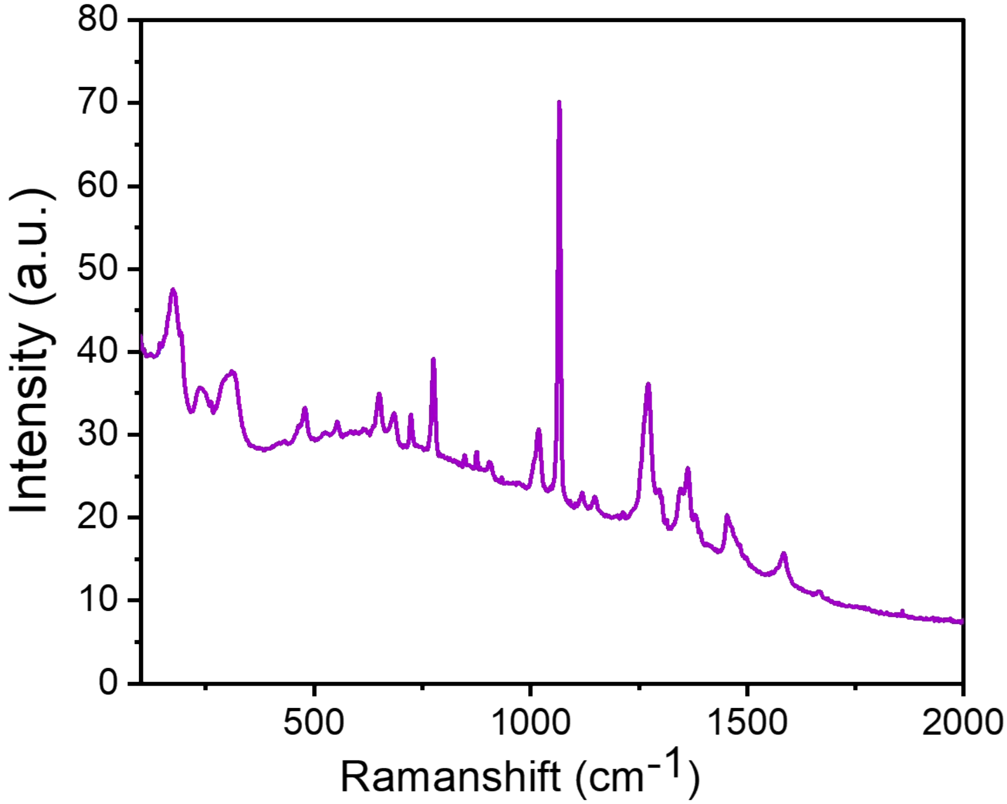

Fig. S11. Raman spectrum of ZIF-9@PVDF membrane showings Co-N bands at 468 cm^{-1}, shows its structural integrity after oil-water separation.

Table S8 Filtration performances of state-of the art membranes reported in the literature compared to this study for water-in-oil emulsions

Membrane	**Separation efficiency**	**Adsorption capacity (%)**	**Ref**
PVDF/SiO2-TMS - trimethylsiloxane	-	6.5	1
SiO_2-NP-decorated PVDF	99.95	-	2
CR-PBZ@CM	99.94	120	3
PBZ-SiO_2@MS	99.78	82	4
Fluorinated SiO_2-sprayed PVDF membrane	99.94	-	5
ZnO-Co_3O_4 overlapped membrane	99.97	-	6
s-kaolin particles modified PAN composite membra	95	35	7
Tannin-metal complex@polyvinylidene fluoride (TA-Fe@PVDF)	99.5	-	8
PVDF/PDMS	99.81	-	9
Ultra-high molecular weight polytethylene	-	45	10
ZIF-9-III@PVDF	99.5	400	Current Work

References:

[1] J. Ju, T. Wang, Q. Wang, Journal of Applied Polymer Science 2015, 132.

[2] C. Wei, F. Dai, L. Lin, Z. An, Y. He, X. Chen, L. Chen, Y. Zhao, Journal of Membrane Science 2018, 555, 220.

[3] C.-T. Liu, P.-K. Su, C.-C. Hu, J.-Y. Lai, Y.-L. Liu, Journal of Membrane Science 2018, 546, 100.

[4] Y. Peng, Y. Liu, J. Dai, L. Cao, X. Liu, Separation and Purification Technology 2020, 240, 116592.

[5] J. Lin, F. Lin, R. Liu, P. Li, S. Fang, W. Ye, S. Zhao, Separation and Purification Technology 2020, 231, 115898.

[6] N. Liu, X. Lin, W. Zhang, Y. Cao, Y. Chen, L. Feng, Y. Wei, Scientific Reports 2015, 5, 9688.

[7] T. Zhang, C. Zhang, G. Zhao, C. Li, L. Liu, J. Yu, F. Jiao, Colloids and Surfaces A: Physicochemical and Engineering Aspects 2020, 602, 125158.

[8] J. Yang, L. Wang, A. Xie, X. Dai, Y. Yan, J. Dai, Surface and Coatings Technology 2020, 389, 125630.

[9] W. Miao, D. Jiao, C. Wang, S. Han, Q. Shen, J. Wang, X. Han, T. Hou, J. Liu, Y. Zhang, Journal of Water Process Engineering 2020, 34, 101121.

[10] S. Sun, L. Zhu, X. Liu, L. Wu, K. Dai, C. Liu, C. Shen, X. Guo, G. Zheng, Z. Guo, ACS Sustainable Chemistry & Engineering 2018, 6, 9866

Table S9: Comparative study of contact angle measurements and application of hydrophobic MOFs from literature.

S. No.	MOF	Linker	Hydrophobicity Response	Contact Angle	(Ad)/Absorp-tion Capacity	Remarks	Ref.
1	HFGO@ZIF-8	Highly Fluorinated Graphene Oxide (HFGO)	HFGO	162°-0°	150-600 wt%	Composite Material	[1]
2	UHMOF-100	4,4'{[3,5-bis(trifluoromethyl) phenyl]azanediyl}dibenzoic acid (H_2L)	H_2L	176°	40–70 wt%	Membrane Material	[2]
3	NMOF-1	dialkoxyoctadecyl-oligo-(*p*-phenyleneethynylene) dicarboxylate (H_2**OPE-C$_{18}$**)	**H_2OPE-C$_{18}$**	160°–162°	102 $cm^3\ g^{-1}$ (C_6H_6)	Powder	[3]
4	ZIF-67 derived carbon sponge	2-Methylimidazole	Hydrophobic Functional Groups	---	67 g g^{-1} (Soybean oil)	Magnetic Carbon Sponge	[4]
5	ZIF-8/CN foam	2-methylimidazole	Surface Roughness & Blocked Nitrogen	135°	58 wt%	Carbon Nitride Foams	[5]

			Sites				
6	ZIF-8-Sponge	2-methylimidazole	Surface Roughness & Blocked Hydrophilic Sites	120°	74–145 times of its own weight	Sponges	[6]
7	ZIF-7-array & ZIF-7-300	Benzimidazole & 2-methylimidazole	ZIF-7 & Micro/Nanoscale Structure of MOF array coatings and	154.7 ° 151.3 °	---	Array Coatings	[7]
8	UPC-21	H_4L[8]	H_4L	145 ± 1°	196.5 cm^3 g^{-1} at 273 K (C_2H_2)	Crystals	[9]
9	OPA-UiO-66-SO3H &OPA-PCN-222	2-$NaSO_3$-H_2BDC tetrakis(4-carboxyphenyl)-porphyrin (H_2TCPP)	Post synthetic modification (PSM) by n-octadecylphosphonic acid (OPA)	162° & 157°	---	Solid Material	[10]
10	JUC-150@PDMS mesh	Pyrazine	PSM by Polydimethyl-siloxane (PDMS)	143.6 °	---	Mesh	[11]
11	HZIF-8, NZIF-8 & CZIF-8	2-methylimidazole	Polystyrene Template	97°, 67° & 74°	450 wt% Dichloromethane	Powder	[12]
12	MF-ZIF-8-Sponge	2-methylimidazole	Rough and Hydrophobic	140°	3800 wt%	Sponge	[13]

			ZIF-8 Layer				
13	ZIF-8@rGO@Sponge	2-methylimidazole	ZIF-8@rGO & Sponge Roughness	171°	1400~2900 wt%	Sponge	[14]
14	MS-CMC-HPU-13	2-(5-pyridin-4-yl-2*H*-[1,2,4]triazol-3-yl)pyrimidine	2-(5-pyridin-4-yl-2*H*-[1,2,4]triazol-3-yl)pyrimidine	126.1 – 127.1 °	13,000%	Sponge	[15]
15	MOF(1) & MOF(2)	Imidazole-4,5-dicarboxylic acid, bpy and py	Alkylpyridyl groups	129° & 139°	---	Nanosheets & Powder	[16]
16	S-MIL-101(Cr) S-HKUST-1 S-UiO-66 S-ZIF-67	terephthalic acid, benzene-1,3,5-tricarboxylate, 2-Methylimidazole and Octadecylamine	Octadecylamine	156± 1° 155± 1° 154± 1° 151± 1°	142-399 wt% 118-325 wt % 125-281 wt % 122-341 wt %	Powders	[17]
17	UPC-29	H_2L_1 (consider ref.)	H_2L_1	178± 1°	---	Crystals	[18]
18	ZIF-8-SLE meshes	2-methylimidazole & 5, 6-dimethyl-benzimidazole	5, 6-dimethyl-benzimidazole	141.6 ±2°	---	Mesh	[19]
19	Co-MOFs/CF	terephthalic acid	Carbon Foam, Surface Roughness of Co@C/CF	156 °	85 to 200 times its own weight	Hybrid Monolith	[20]

20	ZNM-SSM-2000 & ZNM-SSM-500	Benzimidazole	$Zn_2(bIm)_4$ nanosheet material & Surface Roughness	152.5° & 140°	---	Stainless Steel Meshes	[21]
21	PDMS/Ti MOFs @cotton fabric	2-aminoterephthalic acid	PDMS & Roughness of Fabric Surface	154.7 ± 0.7°	---	Cotton Fabric	[22]
22	HKUST-1 on copper substrates	Trimesic acid (H_3BTC)	Trapped oil of Nano/Micro Structure	152 ± 2.5° (Under Hexane)	---	Mesh	[23]
23	PS@ZIF-8 foam	2-methylimidazole	Polystyrene (PS)	154°	2400-3900 wt%	Monolithic Foam	[24]
24	Zr(Hf)-UiO-66-SH-y	2,5-Dimercapto-1,4-benzenedicarboxylic acid	y=fluoroalkyl	154.4 ± 1°	---	Powder	[25]
25	Eu-bdo-COOH AM-rGA	H_4bdo = 2,5-bis(3,5dicarboxylphenyl)-1,3,4-oxadiazole	Amylamine	32° 142°	4517-14,728 wt %	Aerogel	[26]
26	FG-HKUST-1	Trimesic acid (H_3BTC)	Fluorinated Graphene	147 ± 3°	226-804 wt %	Composite Sponge	[27]
27	Ni/C600	1,3,5-benzenetricarboxylic acid	Disappearance of Hydrophilic groups by	140.3°	---	Aerogel	[28]

			pyrolysis				
28	UiO-66-NH-C18	2-aminoterephthalic acid, triethylamine and octadecanoyl chloride	Hydrophobic alkyl chains	151.7 °.	32.3 to 66.1 g/g	Powder	[29]
29	MIL-100(Fe)	Trimesic acid (H_3BTC)	Residual alkyl chain	179°	---	Powder	[30]
30	UiO-66-NH_2@NWF-g-MAH	BDC-NH_2	Hydrophobic nano- thick MOF coating	138.7 ° at LBL-4	---	Coating Material	[31]
31	HKUST-1/HDT/CF	Trimesic acid (H_3BTC)	Hexadecanethiol	162.91°	---	Metal Foam	[32]
32	ZIF-8-coated SSMs (ZFCMs)	2-methylimidazole	ZIF-8	153.1 ° ± 2.0	---	Stainless-Steel Meshes	[33]
33	ZIF-L coated meshes	2-methylimidazole	Rough micro-/nano hierarchical surface	160°	---	Mesh Films	[34]
34	CuBTC/Cu$(OH)_2$ NWM-PDMS	1,3,5-benzenetricarboxylic acid (H_3BTC)	Methylpolysiloxane (PDMS)	156.2 °	---	Metal Mesh	[35]
35	SH-UiO-66@CFs	2-trifluoroacetamidoterephthalic acid	2-trifluoroacetamido terephthalic acid	163°	More than 2500 wt %	Cotton Fiber	[36]

36	UiO-66-F	$BDC-NH_2$ & Pentadecafluoro-octanoylchloride	Pentadecafluoro-octanoylchloride	145°	163-351 wt%.	Powder	[37]
37	UiO-66-1F(10) @PDA@sponge	4-fluorobenzoic acid	4-fluorobenzoic acid	150◦	50.5-107.8 g/g	Sponge	[38]
38	kgd-Zn@MF	3,5- bis((3’-carboxylbenzyl)oxy)benzoic acid (H_3bcoba)	kgd-Zn seeds	130◦	5077–1378 wt%	Foam	[39]
39	ZIF-8@SA @Sponge	2-methylimidazole	Stearic acid (SA)	140.8 °	30.26-115.35 times its own weight	Sponge	[40]
40	MFS-PC-MIL-100 sponge	Trimesic acid (H_3BTC)	MOF derived porous carbon	145 ± 6◦	10–17 times its own weight	Carbon Sponge	[41]
41	ZIF-8@PLA	2-methylimidazole	ZIF-8	145◦	15 - 30 times its own weight	Aerogel	[42]
42	ZIF-9@PVDF	Benzimidazole	ZIF-9	144	400 wt%	Membrane	current work

References:

[1] K. Jayaramulu, K. K. R. Datta, C. Rösler, M. Petr, M. Otyepka, R. Zboril, R. A. Fischer, *Angewandte Chemie International Edition* **2016**, *55*, 1178.

[2] S. Mukherjee, A. M. Kansara, D. Saha, R. Gonnade, D. Mullangi, B. Manna, A. V. Desai, S. H. Thorat, P. S. Singh, A. Mukherjee, S. K. Ghosh, **2016**, *22*, 10937.

[3] S. Roy, V. M. Suresh, T. K. Maji, *Chemical Science* **2016**, *7*, 2251.

[4] K.-Y. Andrew Lin, H.-A. Chang, B.-J. Chen, *Journal of Materials Chemistry A* **2016**, *4*, 13611.

[5] D. Kim, D. W. Kim, O. Buyukcakir, M.-K. Kim, K. Polychronopoulou, A. Coskun, *Adv. Funct. Mater.* **2017**, *27*, 1700706.

[6] H. Zhu, Q. Zhang, B.-G. Li, S. Zhu, *Advanced Materials Interfaces* **2017**, *4*, 1700560.

[7] G. Zhang, J. Zhang, P. Su, Z. Xu, W. Li, C. Shen, Q. Meng, *Chem. Commun.* **2017**, *53*, 8340.

[8] M. Zhang, L. Zhang, Z. Xiao, Q. Zhang, R. Wang, F. Dai, D. Sun, *Scientific Reports* **2016**, *6*, 20672.

[9] M. Zhang, X. Xin, Z. Xiao, R. Wang, L. Zhang, D. Sun, *Journal of Materials Chemistry A* **2017**, *5*, 1168.

[10] Y. Sun, Q. Sun, H. Huang, B. Aguila, Z. Niu, J. A. Perman, S. Ma, *Journal of Materials Chemistry A* **2017**, *5*, 18770.

[11] Z. Kang, S. Wang, L. Fan, Z. Xiao, R. Wang, D. Sun, *Materials Letters* **2017**, *189*, 82.

[12] P. Jing, S.-Y. Zhang, W. Chen, L. Wang, W. Shi, P. Cheng, *Chemistry – A European Journal* **2018**, *24*, 3754.

[13] Z. Lei, Y. Deng, C. Wang, *Journal of Materials Chemistry A* **2018**, *6*, 3258.

[14] J. Gu, H. Fan, C. Li, J. Caro, H. Meng, *Angewandte Chemie International Edition* **2019**, *58*, 5297.

[15] Z. Xu, J. Wang, H. Li, Y. Wang, *Chemical Engineering Journal* **2019**, *370*, 1181.

[16] J.-H. Deng, Y.-Q. Wen, J. Willman, W.-J. Liu, Y.-N. Gong, D.-C. Zhong, T.-B. Lu, H.-C. Zhou, *Inorganic Chemistry* **2019**, *58*, 11020.

[17] M.-L. Gao, S.-Y. Zhao, Z.-Y. Chen, L. Liu, Z.-B. Han, *Inorganic Chemistry* **2019**, *58*, 2261.

[18] M. Zhang, B. Guo, Y. Feng, C. Xie, X. Han, X. Kong, B. Xu, L. Zhang, *Inorganic Chemistry* **2019**, *58*, 5384.

[19] X. Du, L. Fan, M. Zhang, Z. Kang, W. Fan, M. Wen, Y. Zhang, M. Li, R. Wang, D. Sun, *Materials Research Bulletin* **2019**, *111*, 301.

[20] X. Ge, W. Qin, H. Zhang, G. Wang, Y. Zhang, C. Yu, *Nanoscale* **2019**, *11*, 12161.

[21] C. Ma, Y. Li, P. Nian, H. Liu, J. Qiu, X. Zhang, *Separation and Purification Technology* **2019**, *229*, 115835.

[22] Y. Yang, W. Huang, Z. Guo, S. Zhang, F. Wu, J. Huang, H. Yang, Y. Zhou, W. Xu, S. Gu, *Cellulose* **2019**, *26*, 9335.

[23] J. Du, C. Zhou, Z. Yang, J. Cheng, Y. Shen, X. Zeng, L. Tan, L. Dong, *Surface and Coatings Technology* **2019**, *363*, 282.

[24] C. Tan, M. C. Lee, M. Arshadi, M. Azizi, A. Abbaspourrad, *Angewandte Chemie International Edition* **2020**, *59*, 9506.

[25] J. Du, L. Chen, X. Zeng, S. Yu, W. Zhou, L. Tan, L. Dong, C. Zhou, J. Cheng, *ACS Applied Materials & Interfaces* **2020**, *12*, 28576.

[26] T. Sun, S. Hao, R. Fan, M. Qin, W. Chen, P. Wang, Y. Yang, *ACS Applied Materials & Interfaces* **2020**, *12*, 56435.

[27] R. Yogapriya, K. R. D. Kasibhatta, *ACS Applied Nano Materials* **2020**, *3*, 5816.
[28] Y. Su, Z. Li, H. Zhou, S. Kang, Y. Zhang, C. Yu, G. Wang, *Chemical Engineering Journal* **2020**, *402*, 126205.
[29] M. Shi, R. Huang, W. Qi, R. Su, Z. He, *Colloids and Surfaces A: Physicochemical and Engineering Aspects* **2020**, *602*, 125102.
[30] R. Wang, Y. Feng, H. Xu, Y. Zou, L. Fan, R. Zhang, Y. Zhou, *Materials Chemistry Frontiers* **2020**, *4*, 3086.
[31] J. Gao, W. Wei, Y. Yin, M. Liu, C. Zheng, Y. Zhang, P. Deng, *Nanoscale* **2020**, *12*, 6658.
[32] W. Zhang, S. Wei, W. Tang, K. Hua, C.-x. Cui, Y. Zhang, Y. Zhang, Z. Wang, S. Zhang, L. Qu, *New Journal of Chemistry* **2020**, *44*, 7065.
[33] X. Gao, Q. Ma, Z. Jin, P. Nian, Z. Wang, *New Journal of Chemistry* **2020**, *44*, 13534.
[34] T. Chen, A. Lewis, Z. Chen, X. Fan, N. Radacsi, A. J. C. Semiao, H. Wang, Y. Huang, *Separation and Purification Technology* **2020**, *240*, 116647.
[35] J. Zhu, F. Zhao, T. Peng, H. Liu, L. Xie, C. Jiang, *Surface and Coatings Technology* **2020**, *402*, 126344.
[36] R. Dalapati, S. Nandi, C. Gogoi, A. Shome, S. Biswas, *ACS Applied Materials & Interfaces* **2021**, *13*, 8563.
[37] N. Yuan, X.-R. Gong, B.-H. Han, *ACS Applied Nano Materials* **2021**, *4*, 1576.
[38] B. Yang, M. Shi, R. Huang, W. Qi, R. Su, Z. He, *Colloids and Surfaces A: Physicochemical and Engineering Aspects* **2021**, *616*, 126322.
[39] S. Gai, R. Fan, J. Zhang, X. Zhou, K. Xing, K. Zhu, W. Jia, W. Sui, P. Wang, Y. Yang, *Journal of Materials Chemistry A* **2021**, *9*, 3369.
[40] T. Azam, E. Pervaiz, S. Farrukh, T. Noor, *Materials Research Express* **2021**, *8*, 015019.
[41] M. Bauza, G. Turnes Palomino, C. Palomino Cabello, *Separation and Purification Technology* **2021**, *257*, 117951.
[42] Y. Li, Q. Luo, X. Wang, Z. Duan, P. Lu, S. Li, D. Ji, Z. Wang, G. Li, D. Yu, W. Liu, *Separation and Purification Technology* **2021**, DOI: https://doi.org/10.1016/j.seppur.2021.118794118794.